Iron ore interpretation using gravity-gradient inversions in the Carajás, Brazil

Dionísio Uendro Carlos*, VALE S.A./Observatório Nacional/Colorado School of Mines, Leonardo Uieda, Observatório Nacional, Yaoguo Li, Colorado School of Mines, Valéria C. F. Barbosa, Observatório Nacional, Marco A. Braga, Glauco Angeli, and Guilherme Peres, VALE S.A.

Summary

We have interpreted the airborne gravity gradiometry data from Carajás Mineral Province (CMP), Brazil, by using two different 3D inversion methods. Both inversion methods parameterized the Earth's subsurface into prismatic cells and estimate the 3D density-contrast distribution that retrieves an image of geologic sources subject to an acceptable data misfit. The first inversion method imposes smoothness on the solution by solving a linear system that minimizes an depth weighted L_2 model objective function of density-contrast distribution. The second imposes compactness on the solution by using an iterative growth algorithm solved by a systematic search algorithm that accretes mass around user-specified prisms called "seeds". Using these two inversion methods, the interpretation of full tensor gravity gradiometry data from an iron ore deposit in the area named N1 at CMP shows the consistent geometry and the depth of iron orebody. To date, the maximum depth of the iron orebody is assumed to be 200 m based on the maximum depth attained by the deepest well drilled in this study area. However, both inversion results exhibit a source whose maximum bottom depth is greater than 200 m. These results give rise two interpretations: i) the iron orebody may present its depth to the bottom greater than the maximum depth of 200 m attained by the deepest borehole; or ii) the iron orebody may be 200 m deep and the rocks below may be jaspilite whose density is close to that of soft hematite.

Introduction

The Carajás Mineral Province (CMP) is considered a major mineral province of Brazil and represents one of the largest economic metal concentrations in the world (Galarza et al., 2008). Recent technological developments of the moving-platform gravity gradiometers made it feasible to accurately measure the independent components of the gravity gradient tensor. This fact impel airborne gravity gradiometry to come to be a useful tool for interpretating orebodies in a mining district (Carlos et al., 2011). Here, we inverted the full tensor gravity gradiometry data from the N1 area in the CMP by using two different inversion methods: (1) Li (2001), and (2) Uieda and Barbosa (2011). In both methods, the Earth's subsurface is parameterized into a set of 3D prisms whose density contrasts are the parameters to be estimated. The estimates 3D density-contrast distribution in both methods must yield an acceptable data fit and one would expect that they retrieve the image of the orebodies.

Li (2001) inverts multi-component gravity gradiometer data by minimizing the regularizing function subject to data and bound constraints on the density contrasts. This method uses the regularizing function defined as the sum of the squared L_2 norm of the weighted density-contrast distribution and the squares of the L_2 norms of of first-order derivatives of the weighted density-contrast distribution along three axis directions. The recovered 3D density-contrast distribution has minimum structure that depicts a smoothed image of the geologic bodies. To accelerate the inversion, the method also applies a 3D wavelet compression on each row of the sensitivity matrix.

Uieda and Barbosa (2011) invert multi-component gravity gradiometer data by using a search algorithm that does not require the solution of an equation system. In this method the solution grows systematically around user-specified prismatic elements, called 'seeds', with given density contrasts. Each seed can be assigned a different density-contrast value, allowing the interpretation of multiple sources with different density contrasts. This method imposes compactness on the solution using a modified version of the regularizing function proposed by Silva Dias et al. (2009). For fast inversions of a large data set, Uieda and Barbosa (2011) implement a "lazy evaluation" of the sensitivity matrix.

By applying Li's (2001) and Uieda and Barbosa's (2011) methods to the full tensor gravity gradiometry data over the iron ore deposit from the N1 area in Carajás Mineral Province (Brazil), we verify that the density-contrast distributions estimated by both methods match with geological descriptions of the area and the borehole descriptions about the depth of the mineralization. We show that two atlternative interpretations are possible using four boreholes located exactly over a vertical section taken for this analysis. One possibility may suggest that the iron orebody has a depth to the bottom greather than 200 m. Another interpretation may suggest the presence of jaspilite below 200 m.

Geologic Setting

The Carajás Mineral Province is located at the sotheast of the Amazon Craton, northern Brazil and is the second largest one in the world in respect to iron, gold, manganese and copper deposits (Grainger et al., 2008 apud Fabre, et al., 2011). Althoff (2000) divided this province into Carajás and Rio Maria terrains. The Archean rocks

comprise four main units: (1) mafic to felsic granulite-facies rocks (Pium Complex) and undifferentiated tonalitic to granodioritic gnaisses and migmatites (Xingu Complex); (2) metavulcanics and metasediments (Itacaiunas supergroup); (3) mudstones, siltstones and sandstones (Aguas Claras Formation); and (4) Archean evolution ended with the emplacement, in the Itacaiunas supergroup, of a monzogranites and A-type granitoids and the Old Salobo granite. The Itacaiunas supergroup is subdivided into three groups: Grão Para, Salobo and Pojuca. The Group Grão Para, our objective, is composed of bimodal volcanics and iron formation overlain by basic metavolcanics and metasediments containing Mn, Au-Cu and Au-Pt deposits. The Salobo and Pojuca Groups comprise metabasalts, iron formations and clastic sediments containing Cu, Au, Ag and Mo mineralizations.

The morphological expression of the N1 study area in CMP resembles a plateau, where the Carajás Formation has dip angle greater than 45 degrees to subvertical. At N1 area the outcrops consist predominantly of soft hematite (SH), soft latheritic hematite (SH-L) or ore canga (OC). Compact iron ore or hard hematite (HH) occurs in small dimensions in association with SH.

Results

The full tensor airborne gravity gradiometry surveys covered the N1 plateau. This plateau is located at an important structural system named Carajás folds that hosts iron deposits of CMP, which contains jaspilites, soft and hard hematite, circumvented by volcanic mafic rocks (Lobato et al., 2005). Figure 1 shows the observed Gzz component of gravity gradient tensor and the airborne survey flight lines. Here, this data set is used in both inversion methods. The survey area is about 78 km^2 (6.5 km x 12 km). The line spacing is 150 m and the mean flight height is 100 m above the topographic surface.

Li's (2001) and Uieda and Barbosa's (2011) inversion methods were performed on 9053 observations of the Gzz component of gravity gradient tensor. The Gzz component was chosen because the anomalies display a good correlation with the superficial geological mapping. Figure 2 shows the observed and predicted Gzz components obtained by using Li's (2001) and Uieda and Barbosa's (2011) inversion methods.

The observed Gzz component of gravity gradient tensor was corrected for the effect of topography using an estimated density for the region of 2.67 g/cm^3.

In applying Li's (2001) and Uieda and Barbosa's (2011) inversion methods, we used an interpretation model consisting of a grid of 194 x 196 x 40 prisms, totaling

1,288,160 prisms. Each prism has has dimensions of 75 m x 75 m x 75 m aproximately. In both inversion methods, the topography used was SRTM with 90 meters of resolution.
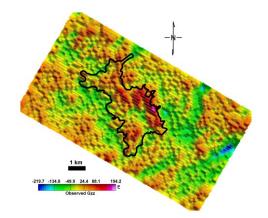

Figure 1: Observed Gzz component of gravity gradient tensor from the N1 area at Carajás Mineral Province (Brazil). The polygon (black line) represents the horizontal projection of the study area (N1 plateau) and the flight lines are shown in gray lines.
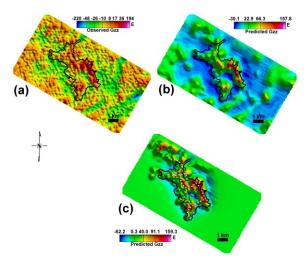

Figure 2: (a) Observed, (b) and (c) predicted Gzz components of the gravity gradient tensor. The predicted Gzz components were produced by Li (2001) in (b) and Uieda and Barbosa (2011) in (c). The polygon (black line) represents the horizontal projection of the N1 plateau and the small white triangules in (c) are the horizontal locations of the seeds required in applying Uieda and Barbosa's (2011) method.

To apply Li's (2001) inversion method we set a zero reference model and lower and and upper bounds for density contrast of 0.0 g/cm^3 and 3.5 g/cm^3, respectively. The length scales in each direction were 150 meters. The algorithm requires a stantard deviation for each datum.

Martinez et al. (2010) used a series of inversions by assigning different values to regularization parameters aiming at estimating the errors in the data. In contrast, we implemented a code based on Galbiatti, et al. (2012) to obtain an estimate of standard deviation of the data. Using our approach this value was 20 Eötvös. For an in-depth review of this inversion method, readers are referred to Martinez et al. (2010).

To apply Uieda and Barbosa's (2011) inversion method, we used a set of 45 seeds whose horizontal locations are shown in Figure 2c (triangles). Following the geologic information about the study area, we assigned a density contrast of 0.75 g/cm^3 to all seeds.
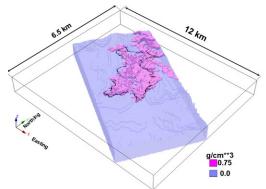

Figure 3: Estimated 3D density-contrast distribution recovered by Uieda and Barbosa's (2011) algorithm. The polygon (black line) represents the horizontal projection of the N1 plateau.
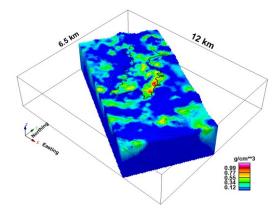

Figure 4: Estimated 3D density-contrast distribution recovered by Li's (2001) algorithm. The polygon (black line) represents the horizontal projection of the N1 plateau.

Figures 3 and 4 show the estimated 3D density-contrast distributions using Uieda and Barbosa (2011) and Li (2001), respectively. We verify that both estimates are consistent with the geologic information from known outcrops of semi compact hematite and canga (a lateritic duricrust of iron hydroxide) as shown in Figure 5.

To verify the quality of both estimates (Figures 3 and 4) in depth, we compare these estimates with the information provided from four boreholes whose horizontal locations coincide with a vertical section (SV26) indicated in Figure 5 by a thick black line.
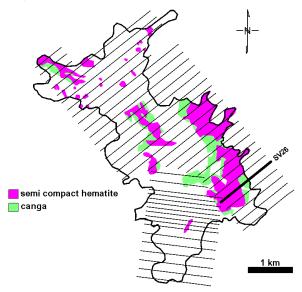

Figure 5: Geological mapping indicates the hematite and canga outcrops. Horizontal locations of all vertical sections (black lines) in the study area. The thick black line indicates the horizontal location of the cross-section SV26 shown in Figures 6 and 7.

The upper panels in Figures 6 and 7 show a detailed map of the observed Gzz component of gravity gradient tensor, the the horizontal projection of the chosen vertical section (black line) and the horizontal locations of the boreholes (A-D). The lower panels in Figures 6 and 7 show the vertical slices of the estimated density-contrast distributions using the two different algorithms. In these lower panels, we can also see the lithological intervals (color ribbons) intersected by each borehole (A-D). The insets on the right of Figures 6 and 7 show the location of the vertical section and the predicted Gzz components of gravity gradient tensor from each inversion.

We note that the deepest borehole (D), whose maximum depth reaches 200 m, comprises alternating layers of hematite and thick jaspilite. In this study area, the hard and soft hematites are the target rocks with densities of 3.6 g/cm^3 and 3.4 g/cm^3, respectively, whereas the jaspilite is a nontarget rock with density of 3.3 g/cm^3. Because the densities of soft hematite and the jaspilite are close, both rocks will produce virtually the same gravity effect.

In a firsr-order analysis, one might consider that the two estimated density-contrast distributions are too different. This conclusion would be based on the nonsmoothed (Figure 6) and smoothed (Figure 7) source images produced by the estimates obtained by using Uieda and Barbosa (2011) and Li (2001), respectively. However, we stress that such features are imposed on the solutions through the regularizing functions used by each inversion method. Hence, these models are different representations of essential features in geology. What's important is that the main density distribution in both density models are consistent with each other and they are also consist with the target rocks intersected in boreholes B-D. The most encouraging aspect of Figures 6 and 7 is that both models (lower panels) overestimate the correct depth of the target body when compared with the deepest borehole D. We interpreted this result by two possibilities. In the first one, we might conclude that iron ore formation (hard and soft hematites) has a depth to the bottom greater than the maximum depth of 200 m attained by the borehole D. In the second possibility, we might conclude that the rock below the maximum depth of 200 m attained by the borehole D is the jaspilite. This second interpretation is based on the negligible difference between the densities of jaspilite and soft hematite.

Conclusions

We have applied two different gravity-gradient inversion methods for interpreting the data from an airborne gravity gradiometry survey flown over the iron orebody from Carajás Mineral Province, northern Brazil. Both inversion methods estimate a 3D density-contrast distribution on a grid of 3D prisms. The estimated density-contrast distributions obtained by both methods and the available geologic information are compatible. By analyzing the inversion results, we concluded that there are two possible interpretations of the estimated density-contrast distributions: (1) the hard and soft hematites may attain a depth to the bottom greater than 200 m or (2) the rock below the depth of 200 m is the jaspilite.
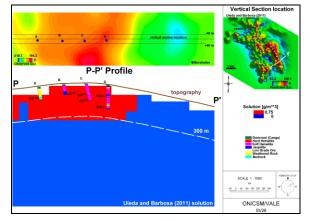
Acknowledgements

Figure 6: Detailed map of the observed Gzz component of the gravity gradient tensor (color map in upper panel) displaying the horizontal projection of the chosen vertical section (black line in upper panel, P-P' profile). Vertical slice of the estimated density-contrast distribution (lower panel) using Uieda and Barbosa's (2011) algorithm and the corresponding predicted Gzz component of the gravity gradient tensor is shown as an inset on the right. The color ribbons in the lower panel represent the lithological intervals intersected by the boreholes A-D.
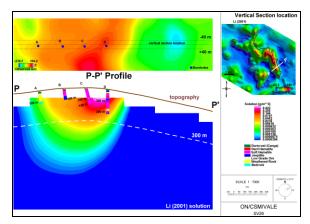

Figure 7: Detailed map of the observed Gzz component of the gravity gradient tensor (color map in upper panel) displaying the horizontal projection of the chosen vertical section (black line in upper panel, P-P'profile). Vertical slice of the estimated density-contrast distribution (lower panel) using Li's (2001) algorithm and the corresponding predicted Gzz component of the gravity gradient tensor is shown as an inset on the right. The color ribbons in the lower panel represent the lithological intervals intersected by the boreholes A-D.

EDITED REFERENCES

Note: This reference list is a copy-edited version of the reference list submitted by the author. Reference lists for the 2012 SEG Technical Program Expanded Abstracts have been copy edited so that references provided with the online metadata for each paper will achieve a high degree of linking to cited sources that appear on the Web.

REFERENCES

Althoff, F., P. Barbey, and A. M. Boullier, 2000, 2.8-3.0 Ga Plutonism and deformation in the SE Amazonian Craton: The Archaean granitoids of Marajoara (Carajás Mineral Province, Brazil): Precambrian Research, **104**, 187–206.

Carlos, D. U., L. Uieda, V. C. F. Barbosa, M. A. Braga, and A. A. S. Gomes, Jr., 2011, In-depth imaging of an iron orebody from Quadrilátero Ferrífero using 3D gravity gradient inversion: 81st Annual International Meeting, SEG, Expanded Abstracts, 902–906.

Fabre, S., A. Nédélec, F. Potrasson, H. Strauss, C. Thomazo, and A. Nogueira, 2011, Iron and surphur isotopes from the Carajás mining province (Pará, Brazil): Implications for the oxidation of the ocean and the atmosphere across the Archaean-Proterozoic transition: Chemical Geology, **289**, 124–139.

Galarza, M. A., M. J. B. Macambira, and R. N. Villas, 2008, Dating and isotopic characteristics (Pb and S) of the Fe oxide-Cu-Au-U-REE Igarapés Bahia ore deposit, Carajas mineral province, Pará state, Brazil: Journal of South American Earth Sciences, 25, 377–397.

Galbiatti, H., M. A. Braga, D. U. Carlos, and R. R. Sousa, 2012, 3D-FTG and Falcon airborne gravity gradiometer systems for iron ore, Brazilian Journal of Geophysics, submitted.

Grainger, C. J., D. I. Groves, F. H. B. Tallarico, and I. R. Fletcher, 2008, Metallogenesis of the Carajás Mineral Province, Southern Amazon Craton, Brazil: Varying styles of Archean through Paleoproterozoic to Neoproterozoic base and precious-metal mineralisation: Ore Geology Reviews, **33**, 451–489.

Li, Y., and D. W. Oldenburg, 1998, 3-d inversion of gravity data: Geophysics, **63**, 109–119.

Li, Y., 2001, 3-D inversion of gravity gradiometer data: 71st Annual International Meeting, SEG, Expanded Abstracts, 1470–1473.

Lobato, L. M., C. A. Rosière, R. C. F. Silva, M. Zucchetti, F. J. Baars, J. C. S. Seoane, F. J. Rios, M. Pimentel, G. E. Mendes, and A. M. Monteiro, 2005, A mineralização hidrotermal de ferro da Província Mineral de Carajás – Controle estrutural e contexto na evolução metalogenética da provincial, *in* Caracterização de Depósitos Minerais em Distritos Mineiros na Amazônia, DNPM-CT/MINERAL-ADIMB, **2**, 20–92.

Martinez C, Y. Li, R. Krahenbuhl, and M. A. Braga, 2010, 3D Inversion of airborne gravity gradiometry for iron ore exploration in Brazil: 80th Annual International Meeting, SEG, Expanded Abstracts, 1753–1757.

Silva Dias, F. J. S., V. C. F. Barbosa, and J. B. C. Silva, 2009, 3D gravity inversion through an adaptative-learning procedure: Geophysics, **74**, no. 3, I9–I21.

Uieda L., and V. C. F. Barbosa, 2011, Robust 3D gravity gradient inversion by planting anomalous densities: 81st Annual International Meeting, SEG, Expanded Abstracts, 820–824.